J. Astron. Space Sci. 17(2), 141–146 (2000)

# GEOTAIL SPACECRAFT OBSERVATIONS OF NEAR-TAIL DIPOLARIZATION AND PLASMA FLOW DURING THE SUBSTORM EXPANSION

**D.-Y. Lee†, K. W. Min, and E. S. Lee**
Physics Department, Korea Advanced Institute of Science and Technology, Taejon 305-701, Korea

*(Received October 15, 2000; Accepted October 31, 2000)*

## ABSTRACT

Some observational features on the July 5, 1995 substorm event are presented using the data from the Geotail satellite which was located at near-Earth plasma sheet, $X_{GSE} \sim -9.6R_E$, and quite close to the onset sector. Near-tail magnetic field reveals the typical dipolarizations starting at $\sim$ 1104 UT until $\sim$ 1113 UT. During the interval, two dipolarizations occur: First dipolarization is not strong and accompanies only weak ($< 150\ km/s$) earthward/dawnward plasma flows, and in the second dipolarization that follows shortly, rather large amplitude magnetic fluctuations are seen, but it initiates with no significant earthward flow. The earthward bursty flow with a maximum speed of $> 450\ km/s$ was observed, but delayed by $\sim$ 1 min with respect to the second dipolarization initiation. These features are in conflict with the flow-braking scenario for the substorm. Rather they fit better in the near-tail current disruption scenario.

*Keywords* : substorm, plasma flow, geotail

## 1. INTRODUCTION

The question of substorm onset and expansion has long been a central issue in the substorm research. One of the key observational features at onset and expansion is the magnetic field dipolarization along with the formation of the so-called substorm current wedge, the auroral arc brightening and the auroral electrojet enhancement. What causes this process has long been a popular theme for active research among substorm scientists.

One popular view in recent days is that the dipolarization at near-tail may be caused by the flow-braking of the bursty bulk flow (BBF) (Fairfield et al. 1999, and references therein). Here the BBF is defined to be a short-duration ($\sim$ 1 - 10 min) high-speed (over 400 km/s) flow. In that scenario, the BBF presumably comes from the midtail reconnection at $\sim$ 25 to 30 $R_E$, and braking of such BBFs at near-tail is to result in opposing currents to the existing cross-tail current and the magnetic flux pileup for dipolarization (Birn et al. 1999). This scenario is basically in line with the popular near-earth neutral line model (Baker et al. 1996), which is still superior to other models in several

†corresponding author

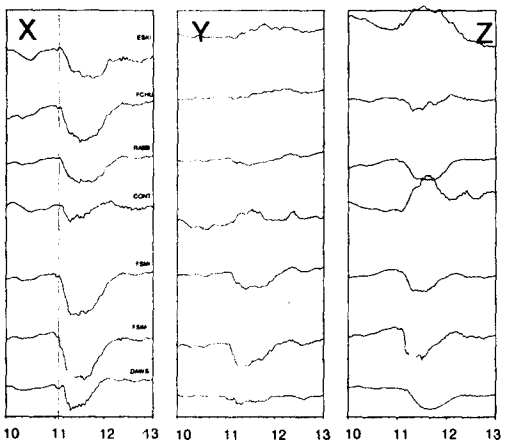


Figure 1. Geomagnetic field variations at stations in the Canadian sector.

aspects. However, it has not been fully demonstrated yet if the dipolarizations are always caused by the earthward BBF-braking without exceptions.

In fact, there exists some observational evidence that the dipolarization can be done with a non-BBF type plasma flow (Lui et al. 1999) which may be explained within the current disruption scenario (Lui 1996). In that scenario, the dipolarization is attributed to some near-tail process which disrupts or reduces the cross-tail current presumably by some type of instability at the substorm onset. The midtail neutral line in that scenario can be considered to be a consequence rather than a cause. One advantage in the current disruption scenario is its flexibility in explaining various types of flows in any direction.

The main purpose of this paper is to report on an substorm observation where the flow pattern at the dipolarization is clearly a non-BBF type. The selected event occurred on July 5, 1995. The magnetic dipolarizations and the associated plasma flow patterns are together examined using the data from Geotail spacecraft while it was passing through the near-tail plasma sheet.

## 2. GROUND GEOMAGNETIC SIGNATURES

Figure 1 shows the geomagnetic variations in $X$, $Y$ and $Z$ components at several ground stations in the Canadian sector for an interval on July 5, 1995. The geographic locations of the stations are shown in Figure 2 together with footpoints of the Geotail and GOES 7 satellites at 11 UT using the Tsyganenko (Tsyganenko 1989) field model. Negative or positive magnetic bays in all components are clearly seen to start around 11 UT. The onset of negative $X$-bay seems to be initiated first at the station FSIM: At first the precursory weak negative bay at $\sim$ 1100 UT, then the major one at $\sim$ 1103 UT. This disturbance propagates in time both longitudinally (eastward and westward) and latitudinally (primarily northward).

The positive and negative bays in $Z$ imply that the westward electrojet channel lies in between ESKI and FCHU, above RABB and FSMI, in between CONT and FSIM, and above DAWS. From the $Y$ component and the Geotail magnetic observations (as discussed in the next section), we believe that this electrojet should be a part of the substorm current wedge system. The downward field-aligned current (FAC) seems to map onto somewhere in between CONT and FSIM in latitude

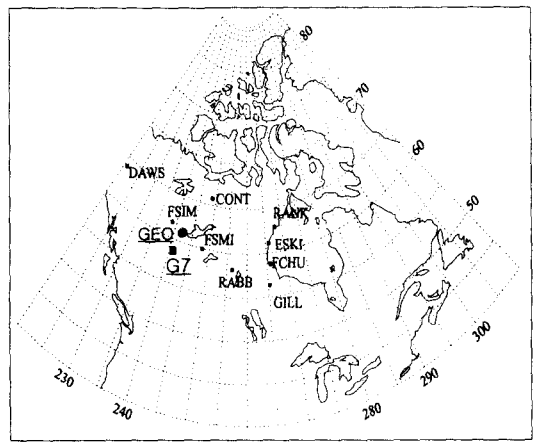


Figure 2. Locations of ground stations in Canadian sector and the footpoints of the two satellites at 11 UT, Geotail and GOES 7 indicated by GEO (circle) and G7 (square), respectively.

around the onset time. This gives negative (westward) *Y*-bay first at FSIM then at FSMI and positive (eastward) *Y*-bay at CONT. This downward sense of the FAC seems to be consistent with the signature observed at Geotail location around similar time. Also, this downward FAC must have propagated eastward, which results in similar *Y*-bays at more eastward stations at little later times, though with much weaker amplitudes. The center of the current wedge must therefore be located westward from FSIM.

## 3. MAGNETOSPHERIC DISTURBANCES

As shown in Figure 2, the Geotail's ionospheric footpoint was very close to FSIM, the ground onset station, around the onset time. The geostationary satellite GOES 7 was located somewhat below Geotail in latitude. While the GOES 7 measured no significant magnetic disturbances around the onset time, strong tail activities were observed by Geotail which was located at $(X, Y, Z)_{GSE} = (-9.6, -4.3, +1.0)R_E$ at 1100 UT. The data of both satellites are shown in Figure 3. The Geotail magnetic field and plasma data were obtained from MGF (Kokubun et al. 1994) and LEP (Mukai et al. 1994) experiments at 3 sec and 12 sec resolutions, respectively. Although both GOES and Geotail satellites were in nearly same MLT at 1100 UT, the disturbance was not observed at GOES 7 probably due to the rather large radial separation of $\sim 4.3R_E$ from Geotail.

Mostly the Geotail was located close to the neutral sheet as can be seen from the magnetic latitude angle $\theta$ (second panel) and ion plasma beta $\beta_i$ (bottom panel). Up until $\sim$ 1100 UT, the $\theta$ decreases gradually, an indication of the magnetic field line stretching during the growth phase. During this, $B_z$ decreases, but the magnitude of $B_x$ slightly decreases, instead of increasing, due to the satellite's movement toward the neutral sheet. The magnitude of total magnetic field is reduced to about 0.3 - 0.4 of the dipole magnetic field there during the growth phase, an indication of the cross-tail current buildup. Then, very weak magnetic fluctuation begins at $\sim$ 1100 UT, and this may be associated with the weak neagtive bay at FSIM at this same time before the major bay at $\sim$ 1103 UT. At Geotail, the major magnetic fluctuation begins at $\sim$ 1104:30 UT, which consequently leads to the dipolarization by cross-tail current reduction. The fluctuation is overall large in its amplitude and it lasts over 8 min. But the largest fluctuation interval with $\delta B \sim B$ is shorter, lasting for

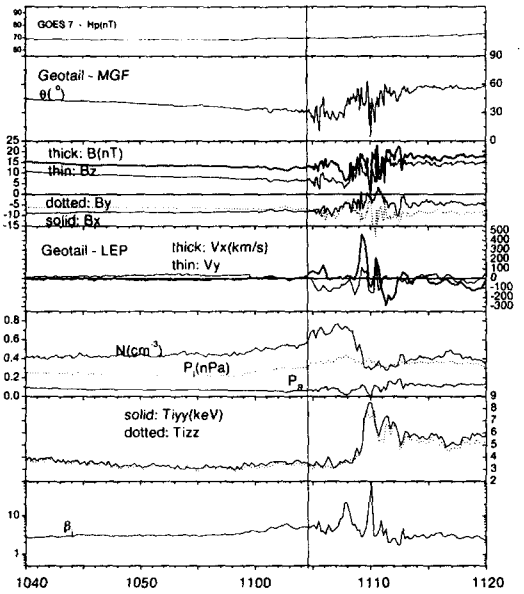


Figure 3. GOES 7 and Geotail data for 1040 to 1120 UT.

$<$ 4 min at the second stage of the dipolarization which begins at $\sim$ 1108 UT. The $B_y$ fluctuation implies the generation of the FAC as a result of the cross-tail current reduction. Although fluctuating, the $B_y$ overall decreases from onset through the end of the largest fluctuation interval, at $\sim$ 1113 UT, implying the primarily dawnward (eastward) magnetic perturbation during the dipolarization. Considering that the Geotail measurement was done in the lower plane of the current sheet, this $B_y$-decrease can be explained by a FAC which flows downward along the field line lying radially outer than the Geotail field line and which maps onto somewhere between CONT and FSIM in the ionosphere (see Figure 2). This is in fact consistent with the earlier interpretation based on the geomagnetic $Y$ component variation in Figure 1.

The Geotail LEP measurements of the plasma flows are also shown in Figure 3. The first dipolarization at 1104:30 UT is accompanied by only weak flows, $\leq 150 km/s$. Also we notice that the second dipolarization starting just before 1108 UT initiates without significant, in particular, earthward flow. The large bursty earthward flow, reaching over 450 km/s in its maximum magnitude, does show up, but is clearly delayed by $\sim$ 1 min from this second dipolarization initiation. Next, a weak tailward flow is accompanied, which is associated with the vanishingly small $B$. Then, after another weaker bursty earthward flow at $\sim$ 1110:30 UT, moderate tailward flow appears beginning at $\sim$ 1111 UT for which $B_z$ is clearly positive. The magnetic field still fluctuates with much reduced-amplitude during this tailward flow period. At this later stage, the flow pattern is overall vortex-like. The hodogram in $V_x - V_y$ space for the time interval [1110:20 - 1116:04] UT is shown in Figure 4. The numbers in the figure represents the time sequences. The flow exhibits the spiral-like eddy structure the magnitude of which decreases in time.

Back in Figure 3, we notice that the ion pressure $P_i$ and number density $N$ increase from $\sim$ 1058 UT. Very interestingly they continue to increase, though with some fluctuations, even after the onset of the magnetic fluctuation. The number density then drops suddenly at around 1109 UT in

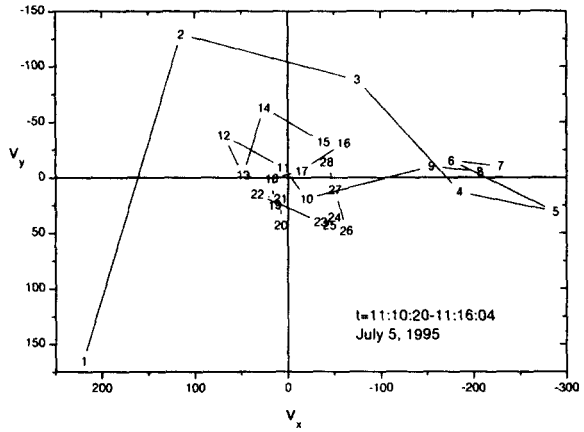


Figure 4. Hodogram of plasma motion in $V_X V_Y$ space for 1110-1116 UT.

coincidence with the appearance of the bursty earthward flow. It also coincides with the rapid rise of the temperature which has remained relatively less changing until this sudden rise. The ion pressure at that time decreases, but not as much significantly as the number density due to the enhancement of the temperature. The magnetic pressure $P_B$ is out of phase with the ion plasma pressure $P_i$. The ion plasma beta $\beta_i$ is overall high, and has an increasing trend toward the onset. It does not simply drop near and right after onset. Rather it fluctuates during the dipolarization period, reaching a local value of >70 near 1110 UT when the $B$ becomes vanishingly small. The $\beta_i$ at later stage eventually reduces below the pre-onset value.

## 4. SUMMARY AND DISCUSSION

In this work, we have used first the ground magnetic data to determine the substorm onset timing and structure. From that, we found that the Geotail satellite was located quite close to the onset sector, and it observed the tail activities with a delay time of ~1 min after the ground onset. The FAC structure between the satellite and ground observations is consistent with each other. Also we have noticed that the onset of the first magnetic dipolarization at 1104:30 UT is accompanied by an earthward flow, but the flow magnitude is not sufficiently high to be classified as the bursty bulk flow (BBF) event. Later the second dipolarization occurs near 1108 UT but with no significant earthward flow. The BBF type flow is observed near 1109 UT, and well associated with the decreasing number density and the increasing temperature as reported in the previous literature (Angelopoulos et al. 1996). Its appearance is however delayed by about a minute with respect to the second dipolarization initiation. These observations serve as a good example showing a clear evidence that the BBF is not a cause of the dipolarization (Lui et al. 1999).

The observed features here resemble in several aspects those of the current disruption scenario suggested by Lui (1996). First, before the current disruption, the magnetic field magnitude at near tail was reduced to ~ 0.3 to 0.4 of the dipole field there, indicating a cross tail current buildup. Then rather large magnetic field fluctuation at expansion occurred which has lasted for a few minutes. While the growth phase is a slow time scale process, the magnetic fluctuation occurs on a rapid time scale shorter than that of MHD. In that regard, the near zero value of the total magnetic field just

before 1110 UT should be simply due to the field fluctuation. Also, the onset location of the current disruption, $X \sim 9.6R_E$, is roughly consistent with many previous reports. The induced electric field (the data not shown here) due to such magnetic field fluctuation should be responsible for the particle energization as represented by the temperature increase. The plasma beta reaches a range of high values for which ion dynamics should be non-adiabatic. All these are consistent with the basic nature of the current disruption scenario.

The most notable candidate for the current disruption has been the cross-field current instability (Lui 1996). The highly stretched tail-like field where ion dynamics is expected to be non-adiabatic seems to be suitable for the excitation of such an instability. Ballooning instability may be another possible mechanism for triggering the current disruption (Roux et al. 1991). The instability is known to be triggered for the high beta plasma as in the plasma sheet configuration during the substorm growth phase (Lee 1999). Further research, in particular, on the nonlinear situation (Hurricane et al. 1999), needs to be done in future to explain the large amplitude fluctuations observed in the current disruption observations.

**ACKNOWLEDGEMENTS:** The CANOPUS instrument array was constructed and is maintained and operated by the Canadian Space Agency for the Canadian scientific community. Geotail magnetic field and plasma data were provided by S. Kokubun and T. Mukai through DARTS at the Institute of Space and Astronautical Science in Japan. This work has been supported by Brain Korea 21 project of Korea Ministry of Education.

## REFERENCES

Angelopoulos, V., Coroniti, F. V., Kennel, C. F., Kivelson, M. G., Walker, R. J., Russell, C. T., McPherron, R. L., Sanchez, E., Meng, C.-I., Baumjohann, W., Reeves, G. D., Belian, R. D., Sato, N., Friis-Christensen, E., Sutcliffe, P. R., Yumoto, K., & Harris, T. 1996, J. Geophy Res, 101, 4967

Baker, D. A., Pulkkinen, T. I., Angelopoulos, V., Baumjohann, W., & McPherron, R. L. 1996, J. Geophy Res, 101, 12, 975

Birn, J., Hesse, M., Haerendel, G., Baumjohann, W., & Shiokawa, K. 1999, J. Geophy Res, 104, 19, 895

Fairfield, D. H., Mukai, T., Brittnacher, M., Reeves, G. D., Kokubun, S., Parks, G. K., Nagai, T., Matumoto, H., Hashimoto, K., Gurnett, D. A., & Yamamoto, T. 1999, J. Geophy Res, 104, 355

Hurricane, O. A., Fong, B. H., Cowley, S. C., Coroniti, F. V., Kennel, C. F., & Pellat, R. 1999, J. Geophy Res, 104, 10, 221

Kokubun, S., Yamamoto, T., Acuna, M. H., Hayashi, K., Shiokawa, K., & Kawano, H. 1994, J. Geomag Geoelectr, 46, 7

Lee, D.-Y. 1999, Geophys Res Lett, 26, 2705

Lui, A. T. Y. 1996, J. Geophy Res, 101, 13, 067

Lui, A. T. Y., Liou, K., Nose, M., Ohtani, S., Williams, D. J., Mukai, T., Tsuruda, K., & Kokubun, S. 1999, Geophys Res Lett, 26, 2909

Mukai, T., Machida, S., Saito, Y., Hirahara, M., Terasawa, T., Kaya, N., Obara, T., Matsuoka, A., Mozer, F. S., & Schmidt, R. 1994, J. Geomag Geoelectr, 46, 669

Roux, A., Perraut, S., Robert, P., Morane, A., Pederson, A., Korth, A., Kremser, G., Aparicio, D., Rodgers, D., & Pellinen, R. 1991, J. Geophy Res, 96, 17697

Tsyganenko, N. A. 1989, Planet Space Sci, 37, 5